Biochimica et Biophysica Acta 1848 (2015) 1849–1859

Contents lists available at ScienceDirect

Biochimica et Biophysica Acta

journal homepage: www.elsevier.com/locate/bbamem

Review

Dynamic regulation of lipid–protein interactions☆

Ashley N. Martfeld [1], Venkatesan Rajagopalan [1], Denise V. Greathouse, Roger E. Koeppe II *

Department of Chemistry and Biochemistry, University of Arkansas, Fayetteville, AR 72701, USA

ARTICLE INFO

Article history:
Received 25 November 2014
Received in revised form 27 January 2015
Accepted 29 January 2015
Available online 7 February 2015

Keywords:
Lipid–protein interaction
Membrane protein
Membrane dynamics
Solid-state nuclear magnetic resonance

ABSTRACT

We review the importance of helix motions for the function of several important categories of membrane proteins and for the properties of several model molecular systems. For voltage-gated potassium or sodium channels, sliding, tilting and/or rotational movements of the S4 helix accompanied by a swapping of cognate side-chain ion-pair interactions regulate the channel gating. In the seven-helix G protein-coupled receptors, exemplified by the rhodopsins, collective helix motions serve to activate the functional signaling. Peptides which initially associate with lipid-bilayer membrane surfaces may undergo dynamic transitions from surface-bound to tilted-transmembrane orientations, sometimes accompanied by changes in the molecularity, formation of a pore or, more generally, the activation of biological function. For single-span membrane proteins, such as the tyrosine kinases, an interplay between juxtamembrane and transmembrane domains is likely to be crucial for the regulation of dimer assembly that in turn is associated with the functional responses to external signals. Additionally, we note that experiments with designed single-span transmembrane helices offer fundamental insights into the molecular features that govern protein–lipid interactions.
This article is part of a Special Issue entitled: Lipid–protein interactions.

Contents

1. Overview . . . 1849
2. Helix motions in voltage-gated channels . . . 1849
3. Helix motions in 7-helix receptors . . . 1851
   3.1. Visual rhodopsin . . . 1851
   3.2. Microbial rhodopsins . . . 1852
4. Dynamics of surface-active peptides . . . 1853
5. Dimerization in relation to dynamics and function . . . 1856
6. Dynamics of individual transmembrane helices . . . 1856
7. Perspective . . . 1857
Conflict of interest . . . 1857
Acknowledgments . . . 1858
References . . . 1858

1. Overview

Dynamic properties as well as time-averaged structural features are crucial for the functions performed by membrane proteins. In this review article, we address the nature and importance of transmembrane helix motions for selected functional membrane proteins and model single-span helical peptides. The collected results reveal that subtle molecular interactions can govern the stabilities of model systems, the resting states of membrane proteins, and the activation of biological function.

2. Helix motions in voltage-gated channels

Although the overall ionic concentration is similar on both sides of a cell membrane, the concentrations of individual ion species vary. A membrane potential on the order of −100 mV can be generated by the charge separation resulting from the pumping of specific ions

☆ This article is part of a Special Issue entitled: Lipid–protein interactions.
* Corresponding author. Tel.: +1 479 575 4976; fax: +1 479 575 4049.
E-mail address: rk2@uark.edu (R.E. Koeppe).
[1] These authors contributed equally.

http://dx.doi.org/10.1016/j.bbamem.2015.01.019
0005-2736/

against their concentration gradients. The cell membrane acts as an insulating barrier separating the charges, with the low dielectric inner hydrophobic core sandwiched on both sides by the high dielectric media of the inside and outside of the cell. The thinness of the hydrophobic section (~27 Å) causes the membrane potential to form a robust electric field reaching values up to 107 V/m, which many membrane proteins use to regulate cell functions. A change in the electric field causes reorientation of electric charges or dipoles within a protein, triggering conformational changes that may regulate protein function. The movement of charges or dipoles induces a "gating current" that can be measured experimentally to obtain direct indications of the conformational changes.

Proteins sense voltage by multiple methods: 1) Polar residues such as Asp, Glu, Arg, Lys and His can reorient in an electric field, a mechanism found to be important in voltage-gated ion channels (Fig. 1A). 2) Side chains with an intrinsic dipole moment such as Tyr may also orientate in the electric field (Fig. 1B). 3) Though not recognized yet as a voltage sensor, the α-helix with its intrinsic dipole can also be a voltage-sensing structure, with the ability to reorient in the field (Fig. 1C). 4) Some proteins contain cavities within which free ions can associate (Fig. 1D). A change in the electric field may move free ions, initiating a conformational change, a mechanism found in Na^+–K^+ pump. The complex molecular structure of the channel causes the field strength near the voltage sensor to be different from the field strength near the lipid bilayer [1].

Voltage-gated Na^+, K^+ and Ca^{+2} channels play crucial roles in excitable cells. Each of these channels contains voltage sensors and a selective ion-conduction pore. Their general structure comprises either four independent protein subunits (K^+ channels) or one long polypeptide containing four homologous domains (eukaryotic Na^+ and Ca^{+2} channels). Each domain contains six transmembrane segments (S1–S6) and a pore loop between segments S5 and S6. The voltage sensor is made up of the first four transmembrane segments, with the conduction pore formed by the last two segments and the pore loop. The channels are arranged symmetrically around a central conduction pore, surrounded by four copies of the voltage sensor. The S4 segment was early recognized as a potential candidate for voltage sensing owing to the arrangement of basic residues (Arg and Lys) at every third position [2]. The first four most extracellular basic residues of S4 and the most intracellular acidic residue of S2 are involved in gating currents [3,4].

Two models of channel function, the sliding helix [5,6] and the helical screw model [7], predict that the S4 segments have a transmembrane orientation and that the positively charged residues within S4 serve as gating charges. The charges would move outward across the membrane in response to depolarization, thereby initiating the activation process. Based on thermodynamic and structural considerations, along with extensive structure-function studies and molecular modeling, the sliding helix and helical screw models propose that the positively charged residues in S4 form ion pairs with negatively charged residues in the neighboring S1, S2 and/or S3 segments [8]. The negative resting membrane potential draws the positively charged residues of S4 inward; upon depolarization, this electrostatic force is relieved, allowing each of the S4 segments to move outward spirally such that each positively charged side chain can form a new ion pair with a negatively charged residue (Fig. 2). This configuration would provide the thermodynamic stability required to allow the gating charges of S4 segment to move within the hydrophobic environment of membrane. Studies on the effects of mutating these charges on the gating current of K^+ channels have directly confirmed the importance of the S4 positive charges and also the highly conserved second negatively charged residue on S2 [3,4] for channel opening.

One of the most important tenets of the sliding helix model is that S4 remains in a transmembrane position as it translocates the gating charges. The intracellular end of S4 is linked covalently to the N-terminal of S5, which forms the outer circumference of the pore. Site specific mutagenesis and gating charge measurements reveal that the S3–S4 linker is on the extracellular side of the membrane in the resting state [9,10]. Real-time fluorescence quenching and energy transfer measurements have confirmed S4 motions. Experiments in which selected Arg-to-Cys mutants within S4 were labeled with methanethiosulfonate (MTS) revealed that the inner Arg/Cys replacements are susceptible to MTS from inside the cell in resting state, and accessible to MTS from outside the cell after depolarization [11,12]. Fluorescent labeling studies indicate that several residues on S4 spiral outward toward a hydrophilic environment during activation. Detailed studies of channels labeled at multiple S4 positions provided evidence for both outward translocation and rotation of S4 up to 180° during activation [13,14].

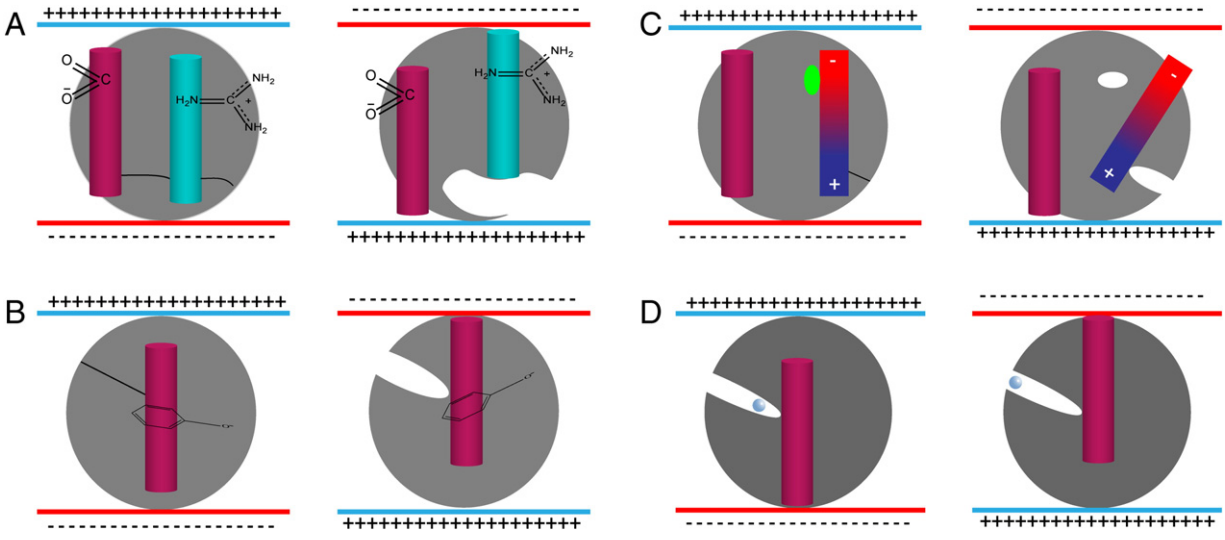

Fig. 1. Possible structures of voltage sensors. The diagram shows a hypothetical protein (gray circle) and the formation of an active site resulting from a voltage-induced conformational change that is regulated by specific regions of the protein (magenta and cyan cylinders). A. Charged amino acids may move within membrane as a response to changes in membrane voltage. The carboxyl and guanidinium groups of Asp and Arg are shown. B. Changes in the field may result in reorientation of an intrinsic dipole such as Tyr. C. An α-helical protein the length of the membrane (red to blue gradient) has a dipole moment that can reorientate when field is changed. The oval attached to the helix represents a fluorophore that may be quenched as a consequence of the conformational change. D. A channel within the protein can redistribute ions (light blue circle) in the direction of the field to initiate a conformational change. Figure redrawn from [1].

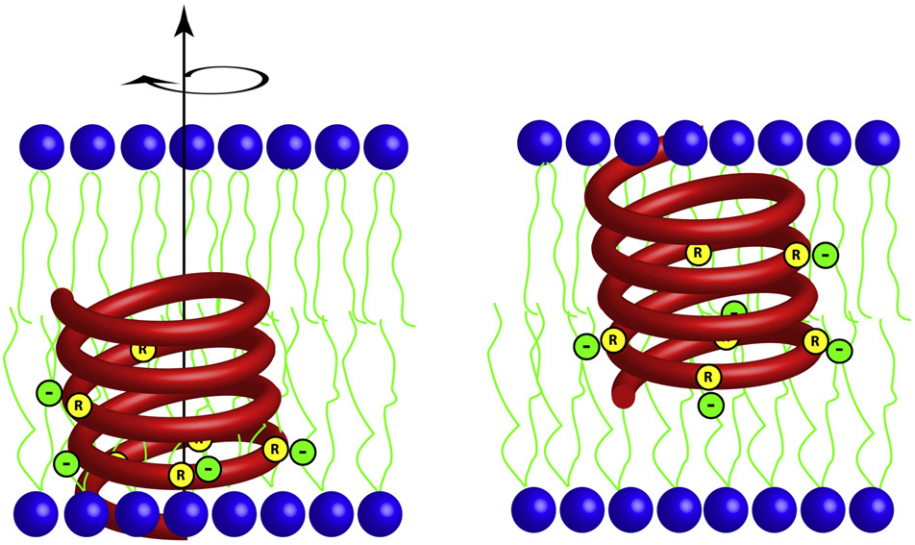

Fig. 2. Sliding helix model of gating. The S4 segment drawn as a spiral of positive charge around it conferred by arginine gating charges (R), which are neutralized by negative charges (−) from surrounding transmembrane segments. The membrane voltage changes cause the S4 segment to move in or out in a spiral path so that the gating charges exchange ion pair partners.

The energetic cost could be considerable for inserting positive charges into a hydrophobic environment. Indeed, synthetic peptides analogous to S4 adopt a surface bound configuration with model membranes [15–17]. The sliding helix model suggests that ion-pairs can stabilize the transmembrane position, with sequential ion pair formation providing a low-energy pathway for movement of the voltage sensor.

Lipid-driven gating and the Helix Tilt-Shift Model. Molecular dynamics (MD) simulations have suggested that the lipid bilayer is perturbed in the vicinity of S4 [18]. Moreover, the surrounding lipid matrix may strongly affect channel activation, as observed for example with KvAP channels [19,20]. Hydrated chloride ions, furthermore, may accompany the S4 arginines [21]. The neighboring lipids, particularly those with anionic or cationic head groups [22], tend to rearrange when the membrane potential is shifted yet, interestingly, the lipids that contact the KvAP channel can be exchanged only when the channel itself is in the open state [20].

A recent "tilt-shift gating model" [23] incorporates environmental parameters and distance constraints from electron paramagnetic resonance (EPR) spectroscopy. The tilt-shift model is characterized as combining a change in helix tilt of ~25° with a downward shift of ~2 Å along the S4 axis from the up state to the down state in the KvAP channel's voltage-sensing domain (Fig. 3). As with a sliding helix, net charge transfer would accompany the S4 vertical movement. It is noted that additional charge transfer may take place as a consequence of changes in the local dielectric constant caused by water entry and subsequent refocusing of the electric field [24,23]. The resulting electric field compression/expansion could influence R133 and K136 in S4. Subsequently, the four arginines (R117, R120, R123, and R126) would drive the tilt toward the down state driven by depolarization. The 3 Å displacement at one end of S4 could be amplified to ~5 Å at the other end of the helix, depending on the position of the hinge point for S4 tilt, and hence would be in agreement with the ~4 Å displacement observed for the KvAP S4–S5 linker by luminescence resonance energy transfer distance measurements [24].

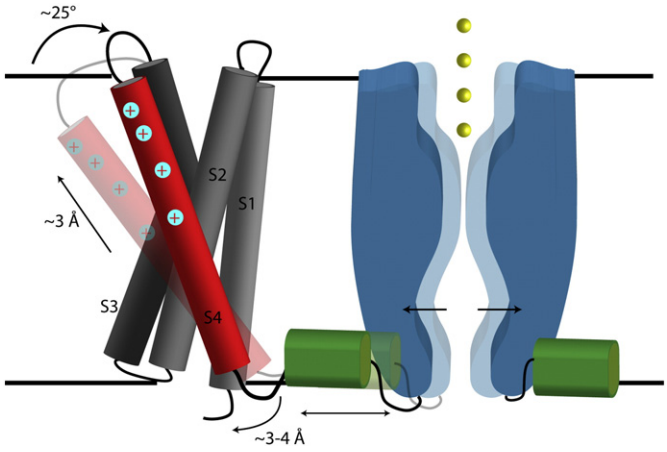

Fig. 3. Tilt-shift model. Cartoon representation of the tilt-shift model on KvAP-VSD. The ~25° tilt and ~3-Å downward shift of S4 could generate a movement of ~3–4 Å of the S4–S5 linker, sufficient to open the pore. Figure redrawn from [23].

Based on the above considerations, helix motions remain a common feature within current models and present understanding of voltage-driven channel gating.

3. Helix motions in 7-helix receptors

G protein-coupled receptor (GPCR) proteins comprise a large family of signaling proteins, each having seven transmembrane helices (7-TM). Rhodopsins comprise a major sub-family of 7-TM proteins with a retinal chromophore at the core of the protein. In vertebrates, rhodopsin functions as a light-activated GPCR to enable vision in low light conditions. Absorption of light by the 11-cis retinal chromophore leads to isomerization to the all-trans conformer. This isomerization in turn causes conformational changes in the TM helices of rhodopsin, allowing the protein to interact with its corresponding G protein, transducin. Conversely, the activation of microbial rhodopsins causes isomerization of all-trans retinal to a cis conformer. Microbial rhodopsins serve a multitude of functions including ion pumps, sensors, and channels. In both vertebrate and microbial rhodopsins, light activation leads to a major conformational change in the transmembrane domain of the protein. Here we discuss dynamic properties of the rhodopsins, as prototypes for the larger 7-TM helix GPCR family.

3.1. Visual rhodopsin

The rhodopsin polypeptide consists of seven transmembrane helices (TM1-7), which vary in length from 20–33 residues, connected by short cytoplasmic and extracellular loops, along with a short amphipathic helix which lies perpendicular to the membrane on the cytoplasmic side. The overall cylindrical shape of rhodopsin results from the packing

of the seven transmembrane helices. The densely packed helices TM1 and TM3 form a stable core in the protein and do not significantly change orientations upon activation. Conversely, the loosely packed helices TM5 and TM6 undergo large conformational changes upon activation [25]. The retinal chromophore is covalently attached to TM7 via a protonated Schiff base. The second extracellular loop (EL2) serves as a cap over the 11-cis retinal binding site. The crystal structure of rhodopsin [26] shows that EL2 folds into a highly ordered structure consisting of two β-strands.

Activation of rhodopsin requires the formation of the intermediates bathorhodopsin, lumirhodopsin, meta-rhodopsin I (Meta I) and meta-rhodopsin II (Meta II). No major conformational changes occur in the bathorhodopsin and lumirhodopsin intermediates. Small conformational changes in the Meta I intermediate prepare the protein to undergo a major conformational change in Meta II, and thereby activate the protein. In dark state rhodopsin, the retinal chromophore sits in a tight binding site at the core of the protein and is attached via a protonated Schiff base linkage with Lys296 on TM7. The counter-ion, Glu113 on TM3, stabilizes the inactive form of the protein. Isomerization of bent 11-cis retinal to the elongated all-trans retinal triggers small local conformational changes as shown in the crystal structures of photorhodopsin, bathorhodopsin, and lumirhodopsin [27].

A cluster of aromatic residues, Phe 261, Trp265 and Tyr268, on the extracellular end of TM6, are associated with its motion. A tight interaction between 11-cis retinal and Trp265 locks TM6 in position in dark state rhodopsin. Solid-state NMR experiments show that retinal moves toward TM5 in the formation of Meta I [28]. This motion places the β-ionone ring of the retinal chromophore in contact with TM5, and leads to changes in the hydrogen bond network between TM3 and TM5 [27]. These changes have been shown to be essential for displacement of Trp265, which rotates toward the extracellular side and allows movement of TM6 (Fig. 4) [29]. Azido-labeling experiments show small changes in the position of TM5 with respect to TM4 in the formation of Meta I [30]. It has been proposed that these changes are a result of the steric clash between the β-ionone ring and TM5 [31]. The clockwise rotation of TM6 occurs during the formation of Meta I and prior to large-scale displacement of TM6 which occurs during the formation of Meta II [31]. Solid-state deuterium NMR studies indicate displacement of Trp265 on TM6 upon receptor activation [32]. The cryo-EM structure of Meta I indicates no change in the intracellular position of TM6; however, changes in the electron density of TM6 in the vicinity of Trp265 could indicate rotation of TM6 with no outward displacement [31]. Azido-labeling studies imply small rotations of TM5 and TM6 in Meta I as a result of retinal isomerization and displacement of Trp265 [30]. Overall, the collective motions serve to activate the functional signaling.

Early experiments indicated the defining motion of rhodopsin activation to be the outward displacement of TM6 (Fig. 5) [33]. Site-directed spin labeling studies were among the first to record this movement [33,34]. The highly conserved Pro267 residue on TM6 is believed to act as a hinge and facilitate motion of TM6 [35]. Small rotational changes in TM5 and TM6 in Meta I therefore set the stage for the large-scale displacement of TM6 in Meta II. A hallmark of Meta II formation is a proton transfer from the protonated Schiff base to Glu113 on TM3. Isomerization induced changes cause the Schiff base counter-ion to change from Glu113 on TM3 to Glu181 on EL2 upon the formation of Meta I [27]. Consequently, Glu113 may be able to move into a more hydrophobic environment and help to drive the deprotonation of the Schiff base [31]. EPR studies indicate that deprotonation of the Schiff base occurs prior to displacement of TM6 whereas proton uptake occurs after TM6 has adopted a tilted conformation [36]. Changes in TM5 orientation in Meta I are followed by the coupled motion of EL2 in Meta II [28]. Rotation of TM6 during Meta I facilitates disruption of the ionic lock between Glu247 on TM3 and Arg135 on TM6 [30,31]. As a result of this disruption, TM6 undergoes an outward displacement of ~5 Å, exposing the G protein binding site and allowing rhodopsin to interact with transducin [36]. Again, the findings reinforce the principle that collective small motions lead to the functional activation.

3.2. Microbial rhodopsins

Microbial rhodopsins are a large family of transmembrane proteins that share a similar 7-TM scaffold structure but exhibit diverse functions. Like visual rhodopsins, microbial rhodopsins contain a retinal chromophore joined to the protein through a protonated Schiff base linkage. Light-induced isomerization of the chromophore in microbial rhodopsins, however, is linked to a variety of different functions including proton pumps, chloride pumps, and cation channels. Unlike the vertebrate visual rhodopsins, microbial rhodopsins directly influence the voltage potential across the membrane. Although microbial rhodopsins carry out a diverse range of functions, it has been hypothesized that all microbial rhodopsins may undergo a similar mechanism of activation.

The most thoroughly investigated and best understood example of microbial rhodopsins is bacteriorhodopsin (BR) [37]. BR is a light driven proton pump found in the membrane of halophilic bacteria. Like most microbial rhodopsins, the absorption of light causes the retinal chromophore to undergo all-trans to 13-cis isomerization, which triggers a series of reactions known collectively as the photocycle [38].

In the ground state of BR, retinal is linked to Lys216 on TM7 through a protonated Schiff base linkage, which is hydrogen-bonded to a key

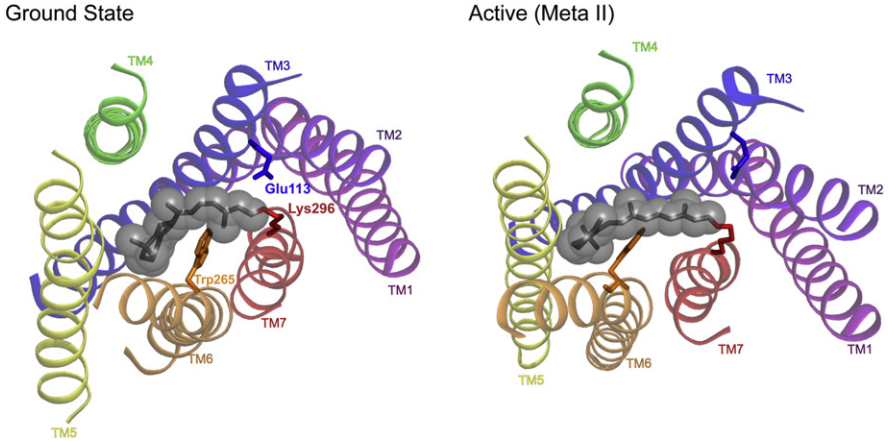

Fig. 4. Retinal binding site in ground state (PDB 1GZM) and active state (PDB 3PXO) rhodopsin. Retinal (gray spheres) is elongated in the 11-cis to -trans isomerization.

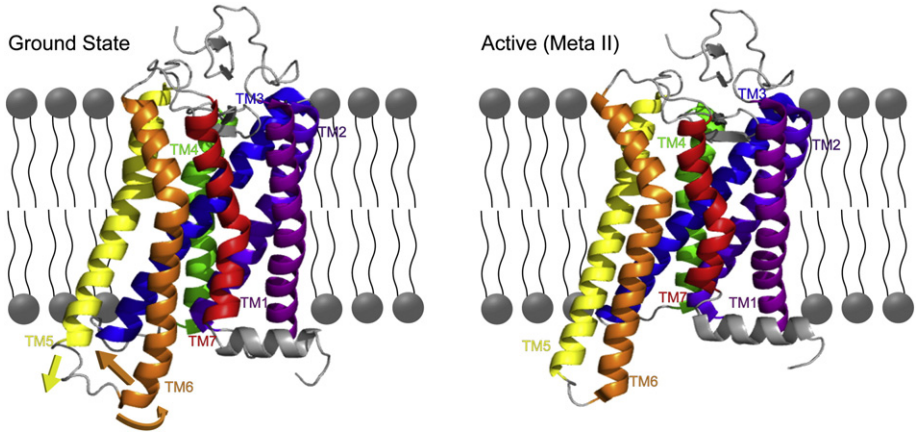

Fig. 5. Side view of visual rhodopsin in ground state (PDB 1GZM) and active state (PDB 3PXO). Motions of TM5 and TM6 associated with rhodopsin activation are shown.

water molecule, which is hydrogen-bonded to Asp85 on TM3. The high pKa (13.5) of the protonated Schiff base and low pKa of Asp85 (2.2) demonstrate how the active site of BR is optimized to prevent protonation of Asp85 by the protonated Schiff base prior to light-induced activation. Like visual rhodopsin, isomerization of the retinal chromophore causes a steric clash in the ligand binding pocket and leads to structural rearrangements in the surrounding residues [38]. Intermediate K is formed when isomerization of the retinal chromophore induces reorientation of the N–H dipole in the Schiff base toward the intracellular side of the membrane. A bound water molecule is displaced, moving Asp85 away from the Schiff base and triggering a sequence of structural rearrangements on the extracellular side of the protein. The second intermediate, L, is formed when the network of water molecules that line the extracellular half of the protein [39] is disrupted and Arg82 on TM3 reorients toward the extracellular side, causing a local inward flex in TM3, bringing Asp85 back into proximity of the Schiff base. These structural changes lead to a perturbation in pKa values of key residues, including a decrease in the Schiff base pKa and increase in the Asp85 pKa, which allows a proton to be transferred to Asp85 upon the transient reorientation toward the Schiff base [40]. Protonation of Asp85 removes the electrostatic attraction between Asp85 and the Schiff base, allowing them to move away from each other and preventing the reverse proton transfer [38]. This event could lead to a relaxation in the flex of TM3 in the M1 intermediate and contribute to the directionality of the proton pumping. In the M2 intermediate, early movement of the backbone carbonyl of Lys216 on TM7 may lead to local unwinding of TM7, creating backbone sites where water molecules could organize along the cytoplasmic end of the protein [41,42].

The M2 intermediate is also characterized by a large outward movement of TM6. One notes that TM6 motions are key events for both rhodopsin and bacteriorhodopsin. In BR, the TM6 movement is triggered by a steric clash between the side chain of Trp182 on TM6 and isomerized retinal. EPR studies show a 50° counter-clockwise rotation accompanied by outward displacement of TM6 [43]. In the ground state, the intracellular side of the protein consists primarily of hydrophobic residues. A large outward motion of TM6 opens the hydrophobic "plug" and allows key residues to be exposed to the cytoplasm, including Asp96 on TM3. The Schiff base is protonated by Asp96, which is subsequently reprotonated from the cytoplasm, thereby activating the proton pump function. When the retinal returns to the all-trans configuration in the O intermediate, the steric clash between retinal and Trp182 on TM6 is relieved and BR returns to the ground state conformation.

Halorhodopsin (HR) is a microbial rhodopsin that functions by pumping chloride ions from the extracellular medium into the cell. The mechanism by which HR functions can be explained by the same Schiff base mechanism through which BR pumps protons out of the cell. A key difference between BR and HR is the replacement of Asp85, a key residue in BR, with Thr85 in HR. The Schiff base counter-ion in HR is a chloride ion that is positioned near Thr85 on the extracellular half of the protein. Isomerization of the retinal causes the protonated Schiff base to move toward the cytoplasmic side of the protein, and the chloride ion follows the positive charge and moves inward through the membrane [44]. Mutation of Asp85 to Thr85 in bacteriorhodopsin confirms that BR and HR utilize a common mechanism, as the bacteriorhodopsin D85T mutant is able to pump chloride ions outward in response to light absorption [45].

Channel rhodopsins are more recently discovered light-induced cation channels found in green algae. The uniqueness of these proteins to activate a cation channel in response to visible light has opened the new and rapidly growing field of optogenetics [46]. A structure of a chimeric channel rhodopsin in the ground state indicates the protein is folded similarly to BR, although structures of the activated channel are not yet available [47]. The chimeric channel rhodopsin structure reveals an electronegative pore, likely the cation-conducting pathway, formed by helices TM1, TM2, TM3, and TM7. Since the majority of negative residues occur on TM2, it is suggested that ion conduction and selectivity may be primarily defined by TM2. In a recent EPR study, conformational changes in TM2 were observed upon light activation [48]. The structure indicates that the cation-conducting pathway is open to the extracellular side, while the cytoplasmic side is occluded by two constriction sites formed by polar residues on TM1, TM2, and TM7. Because the cytoplasmic end of TM1 is highly mobile, it is likely that the movement of TM1 opens the pore that, in the closed state, has been constricted by TM1, TM2, and TM7 [47]. The major conformational change in activation of both BR and HR is the outward tilt of helix TM6, hinged at Pro186. As this proline residue is conserved across channel rhodopsins, it is likely that movement of TM6 is key to the opening of channel rhodopsin as well, though experimental evidence is not currently available. The further engineering of channel rhodopsins is having a significant impact on neuroscience research, in particular by enabling the specific modulation of selected cells within complex neural tissues [46].

4. Dynamics of surface-active peptides

Many membrane-active peptides perform their biological activities by interacting at or near the surface of cell membranes. For example, cationic amino acids in antimicrobial peptides (AMPs) and cell-penetrating peptides (CPPs) promote interactions between the peptide and the lipid head groups and water at the membrane interface. Upon binding at the membrane surface, such peptides may undergo a conformational change from unstructured to an amphipathic α-helix or

β-structure that facilitates insertion, translocation, or disruption of the membrane [49]. Due to their low molecular weight and the inherent fluidity of the lipid membrane, global backbone and segmental motions are common features of membrane-active peptides [50,51]. The conformational plasticity exhibited by many cation-rich peptides is dependent on the environmental conditions and is thought to be important for their diverse activities.

The cationic antimicrobial peptide PGLa (peptidyl-glycine-leucine-carboxyamide, GMASKAGAIAGKIAKVALKAL-NH_2), a member of the magainin family of peptides isolated from the skin of the African frog *Xenopus laevis*, binds initially as an amphiphilic α-helix to bacterial membranes through electrostatic interactions and is able to permeate the lipid bilayer [52]. Orientational constraints obtained from solid-state ^{2}H and ^{19}F NMR measurements of PGLa peptides with selectively labeled Ala-d_3 or ^{19}F-labeled residues in oriented DMPC and DMPC:DMPG bilayers at low peptide concentration (P/L = 1:200) have shown a surface bound α-helical conformation (S-state). The surface orientation is indicated by a tilt angle (τ) of about ≈98° from the bilayer normal, and the lysine side chains extend up toward the water at the membrane interface [52]. At higher peptide concentration (P/L = 1:50), however, PGLa dips into the membrane, aligning into a stable tilted orientation (T-state) with a shallow oblique angle of τ ≈ 125°. No evidence for a state with a fully inserted peptide (I-state) was observed even at high peptide concentration, P/L = 1:20, where the tilt angle remained at τ ≈ 125°. Except under special circumstances, for example in the presence of its synergistic partner magainin 2 [52], or at very low temperatures in the lipid gel phase [53], PGLa does not adopt a fully inserted I-state as observed for some other α-helical peptides such as magainin [54,55]. The unique tilt angle and high stability of the T-state, which change very little over a range of concentrations (P/L = 1:50–1:20) or in the presence of anionic lipids (0–40%), suggest that PGLa may function as a dimer in the membrane [56,52]. These findings are supported by microsecond (1–2 μs) all-atom molecular dynamics simulations that reveal at low concentration (P/L = 1:200) PGLa lies as a monomer on the membrane surface in the proposed S-state, whereas at higher concentration (PL = 1:50) it reorients into a tilted symmetric antiparallel dimer (T-state), with a crossing angle of ≈20–33° and with close contacts involving strong van der Waals interactions between glycine and alanine residues at the dimer interface [57]. The change in peptide alignment, from the S- to T-state, with increasing peptide concentration has been shown to be a general feature of several other amphiphilic helices, including the cell-penetrating peptide MAP and an antimicrobial sequence variant of PGLa $(KIAGKIA)_3$–NH_2, MSI-103 [58].

Solid-state ^{19}F NMR measurements of PGLa selectively labeled with the non-natural amino acid 4-trifluoromethyl-phenylglycine (CF_3-Phg) have provided further evidence for conformational plasticity [59,60]. Like the CD_3 group of deuterium labeled alanine, the CF_3 group, which gives rise to a triplet signal with orientation-dependent dipolar splittings and chemical shifts [61], is rigidly attached at the Cα atom and therefore provides analogous information about the peptide backbone behavior [62]. Dynamic information about the lateral mobility of membrane-bound PGLa was obtained from oriented DMPC [59,52] and DMPC:DMPG [52,53,63] samples in the liquid crystalline phase (>23 °C) aligned with the membrane normal parallel (β = 0) or perpendicular (β = 90) to the magnetic field. The ^{2}H quadrupolar and ^{19}F dipolar splitting magnitudes from PGLa in both the S- and T-states were reduced by a factor of two when changing the sample alignment from β = 0 to β = 90, indicating that membrane-bound PGLa undergoes rapid diffusion about the bilayer normal on a millisecond timescale. In liquid crystalline bilayers, the realignment of PGLa from the S- to the T-state was accompanied by a small change of ~0.6 to ~0.7 in the order parameter "S," which describes the peptide wobble (ranging from 0 for a fully averaged system to 1.0 for complete absence of wobble) [53]. By contrast, S approaches a maximum value of 1.0 at 0 °C for PGLa in gel phase lipids. In gel phase lipids PGLa dimers insert nearly upright into the membrane in the I-state, with a tilt angle of ~170°, and are proposed to be organized into higher-order oligomeric structures that no longer undergo rotational diffusion or wobble motion [53]. At even lower temperatures, −20 to −40 °C, in the subgel phase lipids, powder-like NMR line spectra are observed, indicating that PGLa is completely immobile and no longer has a preferred alignment in the membrane (See Fig. 6, adapted from Fig. 3 of [53]).

Broadened signals observed for oriented samples of ^{19}F labeled PGLa in DMPC at a threshold concentration of P/L = 1:100 suggest that a dynamically averaged intermediate structure, halfway between the S- and T-state, is in fast exchange on the millisecond time scale of the NMR experiment (on the order of the ^{19}F dipolar coupling frequency of up to 10 kHz) [60]. ^{2}H NMR spectra of PGLa with Ala-d_3 labels at 8 positions in fully hydrated DMPC multi-lamellar vesicles (MLVs) confirm that the PGLa peptides are engaged in a dynamic equilibrium of dimerization, albeit at a higher threshold concentration (P/L = 1:50) due to the high level of hydration in MLVs (50%, excess hydration) compared to oriented samples (96% humidity) [52]. The quadrupolar splittings obtained at the threshold concentration are well fit by an arithmetic average between the S- and T-states, indicating a population of 55% S-state and 45% T-state. Solid-state ^{2}H and ^{19}F NMR measurements of PGLa in unilamellar vesicles, hydrated with excess aqueous solution, have shown that the initial adsorption of PGLa to the membrane surface, however, which is accompanied by a change in secondary structure from unordered to α-helical, is a slow process on the NMR timescale [56,52]. Solid-state ^{2}H NMR spectra of PGLa in DMPC and DMPC:DMPG (3:1) multilamellar vesicles show both an isotropic signal from soluble PGLa as well as a quadrupolar doublet from membrane-bound PGLa [52]. An exchange rate of about 10 s^{-1} was estimated from solution state ^{19}F NMR T2-relaxation measurements of PGLa in large unilamellar vesicles [56]. The equilibrium re-alignment of PGLa from a surface-bound S-state to a stable, presumably dimeric, tilted T-state, is influenced by a number of environmental factors, including the peptide concentration, the presence of DMPG, or the hydration level. The dynamic re-alignment is therefore proposed to play a significant role in the functional mechanism of PGLa.

The disulfide constrained β-hairpin antimicrobial peptide PG-1 (protegrin-1, RGGRLCYCRRRFCVCVGR) [64], like PGLa, shows conformational plasticity that depends on its membrane environment. In bacterial-like anionic lipid membranes PG-1 forms oligomeric transmembrane β-barrel structures that result in toroidal pore-like defects in the membrane; however in eukaryotic-like membranes, where the membrane rigidity and negative curvature imparted by cholesterol prevent insertion, it forms β-sheet aggregates on the bilayer surface. In the anionic membranes, it has been proposed that the cationic arginine residues may drag lipid phosphate groups along as they insert into the hydrophobic part of the membrane, thereby facilitating the formation of pore defects [65].

Biological membranes are highly dynamic assemblies in which the lipid molecules undergo fast lateral and uniaxial rotational diffusion, and small peptides and larger proteins frequently experience whole-body and segmental motions, respectively [51]. Of particular interest is the potential insertion of ionizable amino acid residues into the hydrophobic core of lipid bilayers. Two particular arginines in PG-1 were compared [64]. Order parameters from dipolar couplings and chemical shift anisotropies reveal that whereas the backbone of Arg4 on the β-strand is rigid, consistent with a transmembrane oligomerized structure, the backbone of Arg11 in the β-turn region, near the membrane surface and therefore closer to water molecules, is mobile. Although the guanidino side chains of both Arg4 and Arg11 are highly mobile, the side chain of Arg4, heavily constrained by β-strand packing, exhibits larger order parameters (smaller amplitudes of motion) compared to Arg11 [64]. These studies also revealed surprisingly short ^{13}C–^{31}P distances between the Arg guanidinium moiety and the lipid phosphate head groups [65,64]. The even shorter (4.0–6.5 Å) ^{13}C–^{31}P distances observed in the anionic POPE:POPG membranes—compared

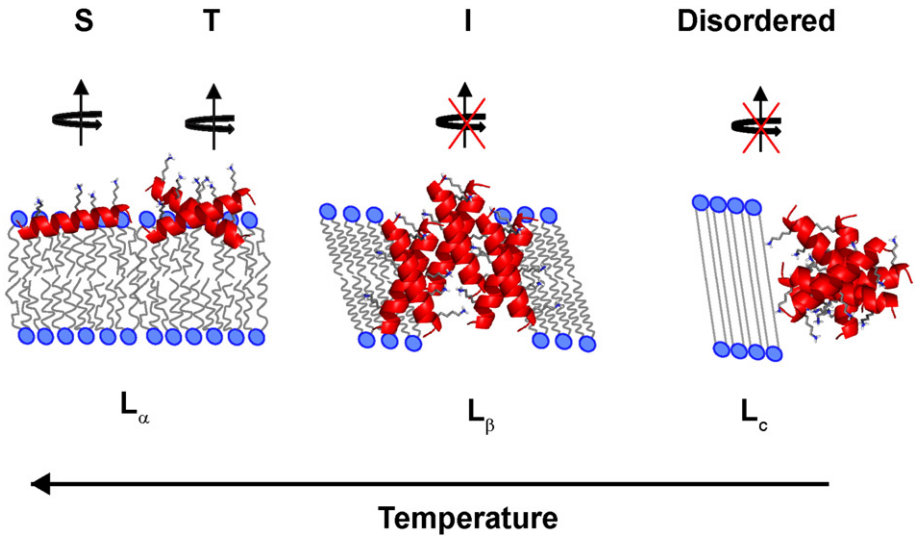

Fig. 6. Four states adopted by PGLa, depending on the temperature and lipid phase. At high temperature (>45 °C) PGLa adopts a monomeric state (S) with the helices aligned parallel to the membrane surface. Close to the melting transition temperature of the lipid acyl chains (45–25 °C) it adopts a tilted state (T), where it is thought to assemble as homodimers. In the lipid gel phase (15–0 °C), PGLa inserts into a nearly upright transmembrane orientation (I), also presumably as dimers which line an aqueous pore and which lacks rotational diffusion. In subgel phase lipids (<0 °C) PGLa is immobile with no defined alignment, even though the lipid molecules remain well oriented. Adapted from [53].

to zwitterionic POPC membranes (6.5–8 Å)—argue for the importance of an ionic interaction. Additionally, the cationic trimethylamine of the POPC head group is expected to repel the guanidinium group and weaken the complex in the neutral membrane. A bidentate complex between the peptide guanidinium ion and two lipid phosphate groups, involving up to 4 hydrogen bonds, could further contribute to the stability (See Fig. 7, adapted from Fig. 10 of [66] and Fig. 9 of [65]). Such an ionic and hydrogen-bond stabilized guanidinium–phosphate complex, as suggested between PG-1 and the lipid head groups, is proposed to be the basis also for the activity of other Arg-rich membrane active peptides and proteins, for example the cell membrane translocation of HIV-TAT [66] and penetratin [67], as well as the gating of the S4 helix of voltage-sensitive potassium channels [18,68].

In the complex amphipathic anisotropic environment of the lipid bilayer, membrane-bound peptides and proteins are subject to additional stresses that could lead to conformational disorder. In contrast to solution NMR, where fast isotropic molecular tumbling is the norm, solid-state NMR spectra of proteins or peptides in membranes often exhibit broad linewidths due to orientation-dependent nuclear spin interactions [69]. By these methods, the membrane peptides PG-1,

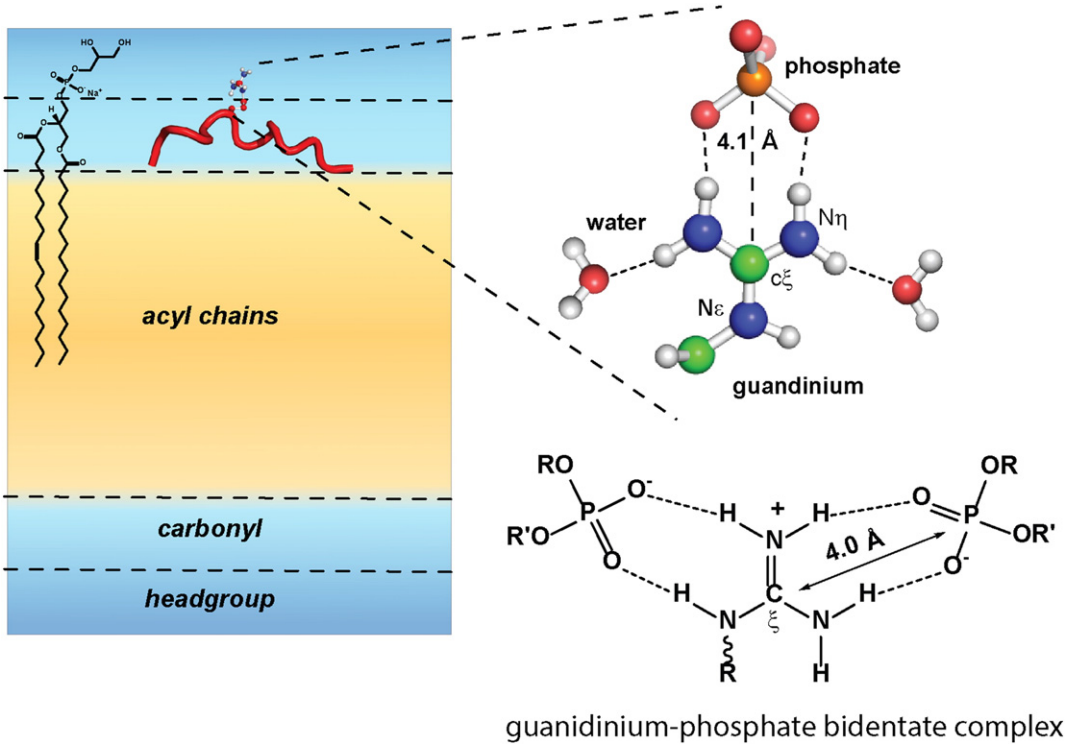

Fig. 7. Model of TAT peptide in phospholipid bilayer. The peptide is located in the glycerol backbone region of the bilayer interface, stabilized by intermolecular hydrogen bonds with lipid phosphates and water [66]. Bidentate guandinium–phosphate complex, stabilized by hydrogen bonds. Adapted from [65].

M2TM (transmembrane domain of influenza M2 protein) and HIV-TAT exhibit differing degrees of conformational disorder. At low temperature (233 K), M2TM and PG-1, which both form oligomers with strong peptide–peptide interactions that promote relatively homogeneous conformations within the membrane, exhibit the least amount of line broadening. By contrast, the near random conformation and extensive peptide–lipid interactions experienced by the monomeric and highly cationic TAT peptide result in larger linewidths and increased conformational disorder. Interestingly, a major source of conformational disorder and line broadening in cationic membrane active peptides is thought to result from the functionally important guanidinium–phosphate ion-pair interactions between Arg residues and the lipid head groups that give rise to multiple side chain conformations, as well as distance and chemical shift distributions. Due to the unique peptide–lipid interactions experienced by Arg-rich peptides, additional line broadening mechanisms are present compared to peptides in a crystalline environment. Overall, dynamic interactions contribute to the functional properties of these classes of membrane-disrupting peptides.

5. Dimerization in relation to dynamics and function

Many signaling cascades invoke the activation of tyrosine kinases, which in turn may depend upon ligand binding and dimerization of a membrane protein receptor. The required physiological sequence of elementary steps as well as the kinetics and regulation of dimer formation are poorly understood [70]. In some cases, the lateral homo- or hetero-dimerization of single-span transmembrane segments may be of critical importance for the biological function [71]. Among such regulated signal-transduction kinases, the epidermal growth factor receptor family (also known as ErbB or HER) is especially prominent in mediating a variety of cellular responses. Sometimes, the activation may be accomplished by means of ligand-induced reorientations of monomers in preformed receptor dimers [72,70]. Furthermore, an intracellular 37-residue juxtamembrane domain, rich in basic residues, plays vital roles for the dimerization and kinase activation [73]. Indeed, the molecular interplay between juxtamembrane and transmembrane domains is likely to be crucial for the regulation of dimer assembly and breakup in response to external signals.

A heterodimer of the transmembrane domains of the ErbB1 and ErbB2 receptor tyrosine kinases is stabilized by intermolecular polar interactions along with hydrogen bonding [71]. It is furthermore speculated that some non-canonical Cα–H···O polar interactions also may contribute to the stabilization of the dimer interface. The sequences SIATGMVGALLLLLVVALGIGLFM (ErbB1) and LTSIISAVVGILLVVVLGVV FGILI (ErbB2) form a stable parallel heterodimer with a crossing angle of about 50° in bilayer-mimicking lipid bicelles of DMPC/DHPC [71]. It is of interest to note that neither corresponding homodimer is observed. The helix–helix contact region just below one membrane/water interface, and significantly above the bilayer center is dominated by polar Thr, Ser and Gly residues. The polar binding helix-interaction surface is close to the lipid head-group region on one side and furthermore is flanked, on the other side, by clusters of Ile/Leu/Met residues, on both strands, that seem to shield the polar helix–helix interface from the lipid environment. (See Fig. 8, adapted from Fig. 3(b) from [71].)

The polar interaction interface for the ErbB1/ErbB2 transmembrane dimer contrasts with the hydrophobic interfaces that sometimes are observed to stabilize interacting pairs of coiled helices in soluble proteins, for example the Leu/Val-dominated interface in the A′α and Jα coiled-coils of the sensor His kinase YF1 [74]. It is evident that a polar interface can promote dimerization within a lipid-bilayer membrane, while a nonpolar interface can promote dimerization in an aqueous environment.

Dimers of transmembrane helices are likely to form by lateral diffusion followed by adjustments of the respective helix orientations. It would be of interest to know the kinetic features of these processes,

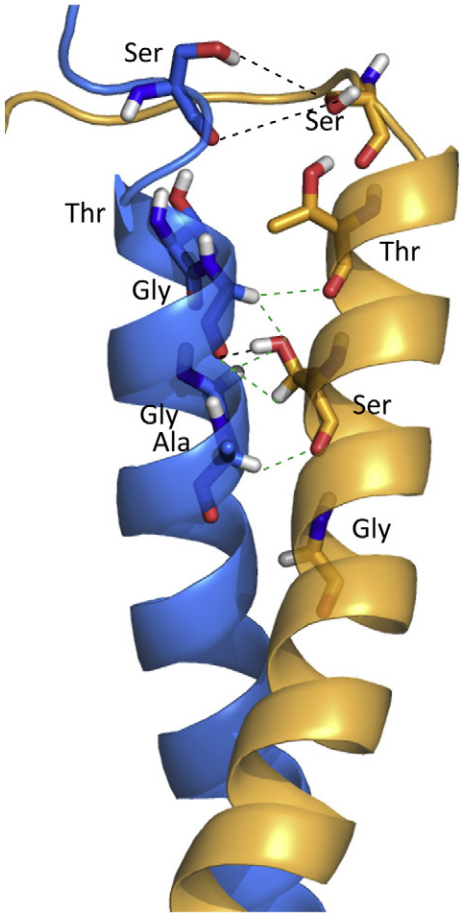

Fig. 8. A model for the polar helix–helix interface of the transmembrane ErbB1–ErbB2 heterodimer. Dimer stability may be provided by classical hydrogen bonds (black dashes) and potentially also by noncanonical C_α–H···O interactions (green dashes). Adapted from Fig. 3(b) of [71].

but little information is available about the time scales. With lateral diffusion within a bilayer membrane likely to be rather slow, the existence of pre-dimers poised for signaling could significantly lower the response time for signal transduction [75,70].

Once a dimer is formed, NMR relaxation times indicate that the individual component helices remain quite rigid [71]. An overall rotational correlation time of about 17 ns has been deduced for a (bicellar) complex consisting of about 70 lipid molecules and the ErbB1/ErbB2 transmembrane dimer, with small flanking segments of about ten residues present N-terminal and C-terminal to the core helices [71].

6. Dynamics of individual transmembrane helices

Model peptides have proven useful for studying fundamental protein–lipid interactions, including dynamic aspects [76–78]. Model systems offer particular advantages for establishing general principles because specific changes in peptide sequence and structure can be made, and direct consequences for interaction with a surrounding lipid membrane can be analyzed. Several membrane proteins, including gramicidin channels, revealed the preferred location of tryptophan residues at a lipid–water interface [79–82]. For model transmembrane peptide design, a core leucine–alanine sequence [83] has been found to render the peptide sensitive to membrane thickness due to hydrophobic mismatch. Then by incorporating “guest” residues within a “host” core sequence, or altering the identities or positions of flanking residues, it becomes feasible to investigate the effects of defined molecular changes on the orientations and dynamics of transmembrane helices, from which inferences for membrane proteins may be deduced.

Rather closely related designed peptides within the GWALP and WALP families have been found to exhibit markedly differing dynamic regimes [84]. Notably, several peptides that possess four interfacial Trp residues, including the "original" WALP peptides [83,85], display extensive dynamic averaging of solid-state NMR observables, including the ^{2}H quadrupolar splittings and the ^{15}N–^{1}H dipolar couplings [84,86]. A related four-Trp peptide, but with two of the Trps displaced by a Leu–Ala "spacer," acetyl-GWALW(LA)$_6$LWLAWA-amide, also resides with the category of "very extensive" dynamics [84].

Remarkably, when two of the tryptophans are replaced, to give the two-Trp peptide, acetyl-GGALW(LA)$_6$LWLAGA-amide (GWALP23) [87,88], the dynamic behavior of the transmembrane helix is significantly moderated into a regime of intermediate motion [84]. Introduction of a single central Arg residue (Fig. 9A) further reduces the global extent of motion, such that the dynamic averaging is further minimized [84]. Interestingly, well-defined transmembrane orientations are observed for both acetyl-GGALWLALALALAR^{14}ALALWLAGA-amide (GWALP23-R14) and acetyl-GGWLALALALAR^{12}ALALALALWGA-amide (W^{3,21}GWALP23-R12), where in each case a helix tilt depends on the bilayer thickness [89]. By contrast, the isomer acetyl-GGALWLALALAR^{12}ALALALWLAGA-amide (GWALP23-R12; Fig. 9B) displays multi-state behavior, with a marked tendency to exit the bilayer [17], perhaps because the Arg is effectively "sandwiched" between the two Trp indole rings. When the Trp indole rings are moved outward and to another face of the helix, it appears that this R12 side chain may be effectively "rescued" from a "cage" to a stable position, where it is accommodated within the transmembrane helix. At the same time, the R14 side chain of transmembrane GW^{3,21}ALP23-R14 (Fig. 9A), although situated between two rings, retains a stable favored position [89]. The larger "cage" spacing and the offset of R14 could be factors that influence the stable TM orientation.

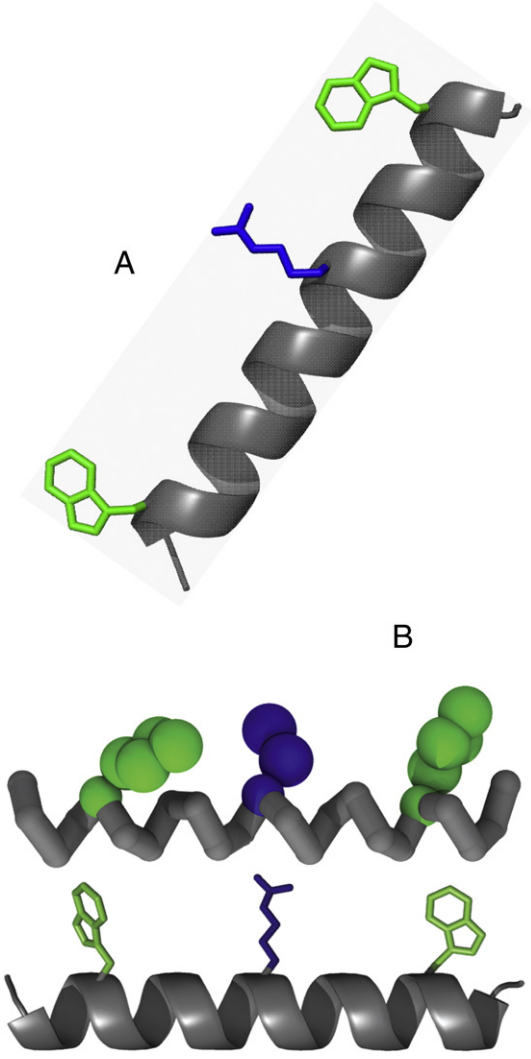

Fig. 9. Models for designed membrane-interacting peptides derived from GWALP23. A. Ribbon model for W^{3,21}GWALP23-R14. B. Coarse-grain and ribbon models for W^{5,19}GWALP23-R12. Adapted from [17] and [89].

When an arginine R12 or R14 in GWALP23 is replaced by lysine, pH-dependent properties are observed for the global helix [90]. Indeed, GWALP23-K12 at low or neutral pH displays multi-state behavior, including a tendency to exit the lipid bilayer, similar to GWALP23-R12 [90]. As the pH is raised from 7 to 9, a dominant tilted transmembrane orientation emerges for GWALP23-K12, mimicking the orientation and global dynamics of GWALP23 itself. The results reflect similar molecular behavior for neutral lysine and neutral leucine, K12 and L12, when "sandwiched" between the W5 and W19 indole rings [90] (See also Fig. 9B.) By contrast, the neutral lysine and neutral leucine confer somewhat different global properties when present at position 14 in GWALP23, away from the Trp residues on the opposite face of the helix. While remaining transmembrane, GWALP23-K14 exhibits pH-dependent properties [90]. At low pH in stacked bilayers of DOPC, GWALP-K14 is rotated and tilted similarly to GWALP-R14, namely about 90° rotated and about 10° more tilted than GWALP23 itself from the bilayer normal. At high pH, with neutral lysine, GWALP23-K14 displays a third state, intermediate between those specified for the non-polar L14 and the charged K14 (or R14). Thus, GWALP23-K14 at high pH displays a smaller tilt similar to GWALP23 but an azimuthal rotation similar to that of GWALP23-R14. This third state for the global helix provides intermediate access of the polar yet neutral lysine residue to the membrane–water interface. The titration analysis indicates a pK_a of ~6.5 for K14 of GWALP23-K14 in DOPC bilayers [90], about four pH units lower than the canonical value for the lysine side chain in aqueous solution.

Further interesting yet incompletely understood correlations between interfacial sequence and transmembrane helix dynamic behavior have been noted. Both GWALP23 and acetyl-GGALY(LA)$_6$LWLAGA-amide (Y^{5}GWALP23) [91] occupy the low to moderate dynamic regime, with a rotational "slippage" $\sigma\rho$ of ~30°–50° about the helix axis in a modified Gaussian analysis [86,78]. By contrast, the inclusion of just one more aromatic residue at Y4 results in very extensive global dynamic averaging [91], wherein $\sigma\rho$ increases to > 90° [78]. (Motions are fast on the NMR time scale.) Interestingly, nevertheless, changing the Y4Y5 sequence to F4F5 moderates the dynamic averaging down to the level observed for GWALP23 itself [78]. Apparently, the removal of polar oxygen atoms and hydrogen-bonding potential to yield F4F5 from Y4Y5 markedly reduces the level of global helix dynamic averaging. For neutral transmembrane helices, the combined results concerning interfacial residue identity and helix dynamics remain somewhat puzzling and await a future explanation.

7. Perspective

Findings to date have established that dynamics and time-dependent properties, in addition to the time-averaged structures, are important determinants and regulators of membrane protein function. While numerous diverse methods have been applied to the arena of lipid–protein interactions, and many individual molecular features have been characterized, the time is ripe for the development of unifying theories to describe the lipid–protein bilayer environment and the regulation of membrane protein function.

Conflict of interest

The authors declare no conflict of interest.

Acknowledgments

Work in the authors' lab has been supported in part by the US National Science Foundation (grant MCB 1327611) and the Arkansas Biosciences Institute.

References

[1] F. Bezanilla, How membrane proteins sense voltage, Nat. Rev. Mol. Cell Biol. 9 (2008) 323–332.
[2] M. Noda, et al., Primary structure of *Electrophorus electricus* sodium channel deduced from cDNA sequence, Nature 312 (1984) 121–127.
[3] S.K. Aggarwal, R. MacKinnon, Contribution of the S4 segment to gating charge in the shaker K^+ channel, Neuron 16 (1996) 1169–1177.
[4] S.A. Seoh, D. Sigg, D.M. Papazian, F. Bezanilla, Voltage-sensing residues in the S2 and S4 segments of the shaker K+ channel, Neuron 16 (1996) 1159–1167.
[5] C.M. Armstrong, F. Bezanilla, Inactivation of sodium channel. 2. Gating current experiments, J. Gen. Physiol. 70 (1977) 567–590.
[6] W.A. Catterall, Voltage-dependent gating of sodium-channels — correlating structure and function, Trends Neurosci. 9 (1986) 7–10.
[7] H.R. Guy, P. Seetharamulu, Molecular-model of the action-potential sodium-channel, Proc. Natl. Acad. Sci. U. S. A. 83 (1986) 508–512.
[8] W.A. Catterall, Ion channel voltage sensors: structure, function, and pathophysiology, Neuron 67 (2010) 915–928.
[9] J.C. Rogers, Y.S. Qu, T.N. Tanada, T. Scheuer, W.A. Catterall, Molecular determinants of high affinity binding of alpha-scorpion toxin and sea anemone toxin in the S3–S4 extracellular loop in domain IV of the Na^+ channel alpha subunit, J. Biol. Chem. 271 (1996) 15950–15962.
[10] M.F. Sheets, J.W. Kyle, R.G. Kallen, D.A. Hanck, The Na channel voltage sensor associated with inactivation is localized to the external charged residues of domain IV, S4, Biophys. J. 77 (1999) 747–757.
[11] N.B. Yang, R. Horn, Evidence for voltage-dependent S4 movement in sodium-channels, Neuron 15 (1995) 213–218.
[12] A. Karlin, M.H. Akabas, Substituted-cysteine accessibility method, Ion Channels 293 (1998) 123–145.
[13] A. Cha, G.E. Snyder, P.R. Selvin, F. Bezanilla, Atomic scale movement of the voltage-sensing region in a potassium channel measured via spectroscopy, Nature 402 (1999) 809–813.
[14] K.S. Glauner, L.M. Mannuzzu, C.S. Gandhi, E.Y. Isacoff, Spectroscopic mapping of voltage sensor movement in the shaker potassium channel, Nature 402 (1999) 813–817.
[15] A. Halsall, C.E. Dempsey, Intrinsic helical propensities and stable secondary structure in a membrane-bound fragment (S4) of the shaker potassium channel, J. Mol. Biol. 293 (1999) 901–915.
[16] K. Mattila, R. Kinder, B. Bechinger, The alignment of a voltage-sensing peptide in dodecylphosphocholine micelles and in oriented lipid bilayers by nuclear magnetic resonance and molecular modeling, Biophys. J. 77 (1999) 2102–2113.
[17] V.V. Vostrikov, B.A. Hall, D.V. Greathouse, R.E. Koeppe II, M.S.P. Sansom, Changes in transmembrane helix alignment by arginine residues revealed by solid-state NMR experiments and coarse-grained md simulations, J. Am. Chem. Soc. 132 (2010) 5803–5811.
[18] J.A. Freites, D.J. Tobias, G. Von Heijne, S.H. White, Interface connections of a transmembrane voltage sensor, Proc. Natl. Acad. Sci. U. S. A. 102 (2005) 15059–15064.
[19] H. Zheng, W.R. Liu, L.Y. Anderson, Q.X. Jiang, Lipid-dependent gating of a voltage-gated potassium channel, nature communications 2, 2011.
[20] E. Faure, C. Thompson, R. Blunck, Do lipids show state-dependent affinity to the voltage-gated potassium channel KvAP? J. Biol. Chem. 289 (2014) 16452–16461.
[21] L. Monticelli, K.M. Robertson, J.L. MacCallum, D.P. Tieleman, Computer simulation of the KvAP voltage-gated potassium channel: steered molecular dynamics of the voltage sensor, FEBS Lett. 564 (2004) 325–332.
[22] E. Madrid, S.L. Horswell, Effect of electric field on structure and dynamics of bilayers formed from anionic phospholipids, Electrochim. Acta 146 (2014) 850–860.
[23] Q.F. Li, S. Wanderling, P. Sompornpisut, E. Perozo, Structural basis of lipid-driven conformational transitions in the KvAP voltage-sensing domain, Nat. Struct. Mol. Biol. 21 (2014) (160- +).
[24] E. Faure, G. Starek, H. McGuire, S. Berneche, R. Blunck, A limited 4 Angstrom radial displacement of the S4–S5 linker is sufficient for internal gate closing in Kv channels, J. Biol. Chem. 287 (2012).
[25] S.O. Smith, Structure and activation of the visual pigment rhodopsin, Annu. Rev. Biophys. 39 (2010) 309–328.
[26] K. Palczewski, et al., Crystal structure of rhodopsin: a G protein-coupled receptor, Science 289 (2000) 739–745.
[27] K.P. Hofmann, P. Scheerer, P.W. Hildebrand, H.-W. Choe, J.H. Park, M. Heck, O.P. Ernst, A G protein-coupled receptor at work: the rhodopsin model, Trends Biochem. Sci. 34 (2009) 540–552.
[28] S. Ahuja, et al., Helix movement is coupled to displacement of the second extracellular loop in rhodopsin activation, Nat. Struct. Mol. Biol. 16 (2009) 168–175.
[29] E. Crocker, M. Eilers, S. Ahuja, V. Hornak, A. Hirshfeld, M. Sheves, S.O. Smith, Location of trp265 in metarhodopsin II: implications for the activation mechanism of the visual receptor rhodopsin, J. Mol. Biol. 357 (2006) 163–172.
[30] S. Ye, E. Zaitseva, G. Caltabiano, G.F.X. Schertler, T.P. Sakmar, X. Deupi, R. Vogel, Tracking G-protein-coupled receptor activation using genetically encoded infrared probes, Nature 464 (2010) (1386-U1314).
[31] M. Eilers, J.A. Goncalves, S. Abuja, C. Kirkup, A. Hirshfeld, C. Simmerling, P.J. Reeves, M. Sheves, S.O. Smith, Structural transitions of transmembrane helix 6 in the formation of metarhodopsin I, J. Phys. Chem. B 116 (2012) 10477–10489.
[32] A.V. Struts, G.F.J. Salgado, M.F. Brown, Solid-state ^{2}H-NMR relaxation illuminates functional dynamics of retinal cofactor in membrane activation of rhodopsin, Proc. Natl. Acad. Sci. U. S. A. 108 (2011) 8263–8268.
[33] D.L. Farrens, C. Altenbach, K. Yang, W.L. Hubbell, H.G. Khorana, Requirement of rigid-body motion of transmembrane helices for light activation of rhodopsin, Science 274 (1996) 768–770.
[34] A.K. Kusnetzow, C. Altenbach, W.L. Hubbell, Conformational states and dynamics of rhodopsin in micelles and bilayers, Biochemistry 45 (2006) 5538–5550.
[35] M.S.P. Sansom, H. Weinstein, Hinges, swivels and switches: the role of prolines in signalling via transmembrane alpha-helices, Trends Pharmacol. Sci. 21 (2000) 445–451.
[36] B. Knierim, K.P. Hofmann, O.P. Ernst, W.L. Hubbell, Sequence of late molecular events in the activation of rhodopsin, Proc. Natl. Acad. Sci. U. S. A. 104 (2007) 20290–20295.
[37] D. Oesterhelt, W. Stoeckenius, Rhodopsin-like protein from purple membrane of *Halobacterium halobium*, Nat. New Biol. 233 (1971) 149–152.
[38] R. Neutze, E. Pebay-Peyroula, K. Edman, A. Royant, J. Navarro, E.M. Landau, Bacteriorhodopsin: a high-resolution structural view of vectorial proton transport, Biochim. Biophys. Acta Biomembr. 1565 (2002) 144–167.
[39] H. Belrhali, P. Nollert, A. Royant, C. Menzel, J.P. Rosenbusch, E.M. Landau, E. Pebay-Peyroula, Protein, lipid and water organization in bacteriorhodopsin crystals: a molecular view of the purple membrana at 1.9 angstrom resolution, Struct. Fold. Des. 7 (1999) 909–917.
[40] M. Andersson, et al., Structural dynamics of light-driven proton pumps, Structure 17 (2009) 1265–1275.
[41] H. Luecke, B. Schobert, J.P. Cartailler, H.T. Richter, A. Rosengarth, R. Needleman, J.K. Lanyi, Coupling photoisomerization of retinal to directional transport in bacteriorhodopsin, J. Mol. Biol. 300 (2000) 1237–1255.
[42] E. Freier, S. Wolf, K. Gerwert, Proton transfer via a transient linear water-molecule chain in a membrane protein, Proc. Natl. Acad. Sci. U. S. A. 108 (2011) 11435–11439.
[43] W.Z. Xiao, L.S. Brown, R. Needleman, J.K. Lanyi, Y.K. Shin, Light-induced rotation of a transmembrane alpha-helix in bacteriorhodopsin, J. Mol. Biol. 304 (2000) 715–721.
[44] J.L. Spudich, O.A. Sineshchekov, E.G. Govorunova, Mechanism divergence in microbial rhodopsins, Biochim. Biophys. Acta Bioenergetics 1837 (2014) 546–552.
[45] J. Sasaki, L.S. Brown, Y.S. Chon, H. Kandori, A. Maeda, R. Needleman, J.K. Lanyi, Conversion of bacteriorhodopsin into a chloride-ion pump, Science 269 (1995) 73–75.
[46] L. Fenno, O. Yizhar, K. Deisseroth, The development and application of optogenetics, in: S.E. Hyman, T.M. Jessell, C.J. Shatz, C.F. Stevens, H.Y. Zoghbi (Eds.),Annual Review of Neuroscience, Vol 34, vol. 34, 2011, pp. 389–412.
[47] H.E. Kato, et al., Crystal structure of the channel rhodopsin light-gated cation channel, Nature 482 (2012) (369-U115).
[48] T. Sattig, C. Rickert, E. Bamberg, H.-J. Steinhoff, C. Bamann, Light-induced movement of the transmembrane helix B in channel rhodopsin-2, Angew. Chem. Int. Ed. 52 (2013) 9705–9708.
[49] Y. Su, S. Li, M. Hong, Cationic membrane peptides: atomic-level insight of structure-activity relationships from solid-state NMR, Amino Acids 44 (2013) 821–833.
[50] P.G. Saffman, M. Delbruck, Brownian motion in biological membranes, Proc. Natl. Acad. Sci. U. S. A. 72 (1975) 3111–3113.
[51] M. Hong, Y.C. Su, Structure and dynamics of cationic membrane peptides and proteins: insights from solid-state NMR, Protein Sci. 20 (2011) 641–655.
[52] P. Tremouilhac, E. Strandberg, P. Wadhwani, A.S. Ulrich, Conditions affecting the re-alignment of the antimicrobial peptide PGLa in membranes as monitored by solid state ^{2}H-NMR, Biochim. Biophys. Acta 1758 (2006) 1330–1342.
[53] S. Afonin, S.L. Grage, M. Ieronimo, P. Wadhwani, A.S. Ulrich, Temperature-dependent transmembrane insertion of the amphiphilic peptide PGLa in lipid bilayers observed by solid state ^{19}F NMR spectroscopy, J. Am. Chem. Soc. 130 (2008) 16512–16514.
[54] S.J. Ludtke, K. He, Y. Wu, H.W. Huang, Cooperative membrane insertion of magainin correlated with its cytolytic activity, Biochim. Biophys. Acta 1190 (1994) 181–184.
[55] H.W. Huang, Action of antimicrobial peptides: two-state model, Biochemistry 39 (2000) 8347–8352.
[56] S. Afonin, R.W. Glaser, M. Berditchevskaia, P. Wadhwani, K.H. Guhrs, U. Mollmann, A. Perner, A.S. Ulrich, 4-fluorophenylglycine as a label for ^{19}F NMR structure analysis of membrane-associated peptides, Chembiochem 4 (2003) 1151–1163.
[57] J.P. Ulmschneider, J.C. Smith, M.B. Ulmschneider, A.S. Ulrich, E. Strandberg, Reorientation and dimerization of the membrane-bound antimicrobial peptide PGLa from microsecond all-atom md simulations, Biophys. J. 103 (2012) 472–482.
[58] J. Burck, S. Roth, P. Wadhwani, S. Afonin, N. Kanithasen, E. Strandberg, A.S. Ulrich, Conformation and membrane orientation of amphiphilic helical peptides by oriented circular dichroism, Biophys. J. 95 (2008) 3872–3881.
[59] R.W. Glaser, C. Sachse, U.H. Durr, P. Wadhwani, A.S. Ulrich, Orientation of the antimicrobial peptide PGLa in lipid membranes determined from ^{19}F-NMR dipolar couplings of 4-cf3-phenylglycine labels, J. Magn. Reson. 168 (2004) 153–163.
[60] R.W. Glaser, C. Sachse, U.H. Durr, P. Wadhwani, S. Afonin, E. Strandberg, A.S. Ulrich, Concentration-dependent realignment of the antimicrobial peptide PGLa in lipid membranes observed by solid-state ^{19}F-NMR, Biophys. J. 88 (2005) 3392–3397.
[61] S.L. Grage, A.S. Ulrich, Orientation-dependent (19)F dipolar couplings within a trifluoromethyl group are revealed by static multipulse NMR in the solid state, J. Magn. Reson. 146 (2000) 81–88.
[62] E. Strandberg, P. Wadhwani, P. Tremouilhac, U.H. Durr, A.S. Ulrich, Solid-state NMR analysis of the PGLa peptide orientation in DMPC bilayers: structural fidelity of ^{2}H-labels versus high sensitivity of ^{19}F-NMR, Biophys. J. 90 (2006) 1676–1686.
[63] M. Ieronimo, S. Afonin, K. Koch, M. Berditsch, P. Wadhwani, A.S. Ulrich, F-19 NMR analysis of the antimicrobial peptide PGLa bound to native cell membranes from bacterial protoplasts and human erythrocytes, J. Am. Chem. Soc. 132 (2010) (8822- +).

[64] M. Tang, M. Hong, Structure and mechanism of beta-hairpin antimicrobial peptides in lipid bilayers from solid-state NMR spectroscopy, Mol. BioSyst. 5 (2009) 317–322.
[65] M. Tang, A.J. Waring, M. Hong, Phosphate-mediated arginine insertion into lipid membranes and pore formation by a cationic membrane peptide from solid-state NMR, J. Am. Chem. Soc. 129 (2007) 11438–11446.
[66] Y. Su, A.J. Waring, P. Ruchala, M. Hong, Membrane-bound dynamic structure of an arginine-rich cell-penetrating peptide, the protein transduction domain of HIV TAT, from solid-state NMR, Biochemistry 49 (2010) 6009–6020.
[67] Y. Su, T. Doherty, A.J. Waring, P. Ruchala, M. Hong, Roles of arginine and lysine residues in the translocation of a cell-penetrating peptide from (13)C, (31)P, and (19)F solid-state NMR, Biochemistry 48 (2009) 4587–4595.
[68] T. Doherty, Y. Su, M. Hong, High-resolution orientation and depth of insertion of the voltage-sensing S4 helix of a potassium channel in lipid bilayers, J. Mol. Biol. 401 (2010) 642–652.
[69] Y. Su, M. Hong, Conformational disorder of membrane peptides investigated from solid-state NMR line widths and line shapes, J. Phys. Chem. B 115 (2011) 10758–10767.
[70] E.G. Hofman, A.N. Bader, J. Voortman, D.J. van den Heuvel, S. Sigismund, A.J. Verkleij, H.C. Gerritsen, P. Henegouwen, Ligand-induced egf receptor oligomerization is kinase-dependent and enhances internalization, J. Biol. Chem. 285 (2010) 39481–39489.
[71] K.S. Mineev, E.V. Bocharov, Y.E. Pustovalova, O.V. Bocharova, V.V. Chupin, A.S. Arseniev, Spatial structure of the transmembrane domain heterodimer of ErbB1 and ErbB2 receptor tyrosine kinases, J. Mol. Biol. 400 (2010) 231–243.
[72] S.J. Fleishman, J. Schlessinger, N. Ben-Tal, A putative molecular-activation switch in the transmembrane domain of ErbB2, Proc. Natl. Acad. Sci. U. S. A. 99 (2002) 15937–15940.
[73] K.W. Thiel, G. Carpenter, Epidermal growth factor receptor juxtamembrane region regulates allosteric tyrosine kinase activation, Proc. Natl. Acad. Sci. U. S. A. 104 (2007) 19238–19243.
[74] R.P. Diensthuber, M. Bommer, T. Gleichmann, A. Moglich, Full-length structure of a sensor histidine kinase pinpoints coaxial coiled coils as signal transducers and modulators, Structure 21 (2013) 1127–1136.
[75] Y. Teramura, J. Ichinose, H. Takagi, K. Nishida, T. Yanagida, Y. Sako, Single-molecule analysis of epidermal growth factor binding on the surface of living cells, EMBO J. 25 (2006) 4215–4222.
[76] M.R. de Planque, B.B. Bonev, J.A. Demmers, D.V. Greathouse, R.E. Koeppe II, F. Separovic, A. Watts, J.A. Killian, Interfacial anchor properties of tryptophan residues in transmembrane peptides can dominate over hydrophobic matching effects in peptide–lipid interactions, Biochemistry 42 (2003) 5341–5348.
[77] P.C.A. van der Wel, N.D. Reed, D.V. Greathouse, R.E. Koeppe II, Orientation and motion of tryptophan interfacial anchors in membrane-spanning peptides, Biochemistry 46 (2007) 7514–7524.
[78] K.A. Sparks, N.J. Gleason, R. Gist, R. Langston, D.V. Greathouse, R.E. Koeppe II, Comparisons of interfacial Phe, Tyr, and Trp residues as determinants of orientation and dynamics for GWALP transmembrane peptides, Biochemistry 53 (2014) 3637–3645.
[79] A.M. O'Connell, R.E. Koeppe II, O.S. Andersen, Kinetics of gramicidin channel formation in lipid bilayers: transmembrane monomer association, Science 250 (1990) 1256–1259.
[80] M. Schiffer, C.H. Chang, F.J. Stevens, The functions of tryptophan residues in membrane proteins, Protein Eng. 5 (1992) 213–214.
[81] C. Landolt-Marticorena, K.A. Williams, C.M. Deber, R.A. Reithmeier, Non-random distribution of amino acids in the transmembrane segments of human type I single span membrane proteins, J. Mol. Biol. 229 (1993) 602–608.
[82] R.E. Koeppe II, Concerning tryptophan and protein-bilayer interactions, J. Gen. Physiol. 130 (2007) 223–224.
[83] J.A. Killian, I. Salemink, M.R. de Planque, G. Lindblom, R.E. Koeppe II, D.V. Greathouse, Induction of nonbilayer structures in diacylphosphatidylcholine model membranes by transmembrane alpha-helical peptides: importance of hydrophobic mismatch and proposed role of tryptophans, Biochemistry 35 (1996) 1037–1045.
[84] V.V. Vostrikov, C.V. Grant, S.J. Opella, R.E. Koeppe II, On the combined analysis of ^{2}H and $^{15}N/^{1}H$ solid-state NMR data for determination of transmembrane peptide orientation and dynamics, Biophys. J. 101 (2011) 2939–2947.
[85] E. Strandberg, S. Özdirekcan, D.T.S. Rijkers, P.C.A. van der Wel, R.E. Koeppe II, R.M.J. Liskamp, J.A. Killian, Tilt angles of transmembrane model peptides in oriented and non-oriented lipid bilayers as determined by ^{2}H solid-state NMR, Biophys. J. 86 (2004) 3709–3721.
[86] E. Strandberg, S. Esteban-Martin, A.S. Ulrich, J. Salgado, Hydrophobic mismatch of mobile transmembrane helices: merging theory and experiments, Biochim. Biophys. Acta 1818 (2012) 1242–1249.
[87] V.V. Vostrikov, C.V. Grant, A.E. Daily, S.J. Opella, R.E. Koeppe II, Comparison of "polarization inversion with spin exchange at magic angle" and "geometric analysis of labeled alanines" methods for transmembrane helix alignment, J. Am. Chem. Soc. 130 (2008) 12584–12585.
[88] V.V. Vostrikov, A.E. Daily, D.V. Greathouse, R.E. Koeppe II, Charged or aromatic anchor residue dependence of transmembrane peptide tilt, J. Biol. Chem. 285 (2010) 31723–31730.
[89] V.V. Vostrikov, B.A. Hall, M.S.P. Sansom, R.E. Koeppe II, Accommodation of a central arginine in a transmembrane peptide by changing the placement of anchor residues, J. Phys. Chem. B 116 (2012) 12980–12990.
[90] N.J. Gleason, V.V. Vostrikov, D.V. Greathouse, R.E. Koeppe II, Buried lysine, but not arginine, titrates and alters transmembrane helix tilt, Proc. Natl. Acad. Sci. U. S. A. 110 (2013) 1692–1695.
[91] N.J. Gleason, V.V. Vostrikov, D.V. Greathouse, C.V. Grant, S.J. Opella, R.E. Koeppe II, Tyrosine replacing tryptophan as an anchor in GWALP peptides, Biochemistry 51 (2012) 2044–2053.